Experimental Time Scale of Gerischer's Distribution Curves for Electron-Transfer Reactions at Semiconductor Electrodes†

F. Willig,*,‡ R. Eichberger,‡ N. S. Sundaresan,‡ and B. A. Parkinson§

Contribution from the Fritz-Haber-Institut der Max-Planck-Gesellschaft, Faradayweg 4-6, D-1000 Berlin 33, West Germany, and Central Research and Development Department, E. I. du Pont de Nemours & Company, Experimental Station E 328/216 B, Wilmington, Delaware 19898. *Received August 16, 1989*

Abstract: Fluorescence decay of adsorbed cresyl violet molecules was measured on n-SnS_2 electrodes where their stationary photoelectrochemical current approached the yield of one electron per absorbed photon. At very low coverage, $\theta \approx 10^{-2}$, the fluorescence decay was faster than 10 ps and was identified with electron injection from excited dye monomers into the wide conduction band of the semiconductor. The reaction path was adiabatic or at least borderline to the adiabatic case. The measurement provides a time scale for Gerischer's distribution curves that are commonly applied in the discussion of electron-transfer reactions at electrodes.

It is now standard practice in electrochemistry to discuss electron-transfer reactions of redox ions at metal[1] and semiconductor electrodes,[1,2] and also of excited dye molecules at semiconductor and insulator electrodes,[3] with the help of Gerischer's distribution curves.

It has been pointed out by several authors[4,5] that Gerischer's distribution curves can be interpreted as representing the energy dependence of the electron-transfer rate constants involving the reduced and the oxidized species, respectively. These rate constants have been derived by several authors from classical[6] and from quantum mechanical models.[7-9] In the classical case the energy dependence of the rate constant[6] and thus the shape of Gerischer's distribution curve is Gaussian. Several quantum mechanical corrections to this shape function have been introduced, in particular those involving the so-called downhill inverted region.[8,10] Only small sections of the complete "rate constant versus energy" distribution curves have been determined for a few redox ions and molecules at electrodes. The measurements addressed rate constants far away from the top of the distribution curves. Convincing time-resolved measurements of rate constants near the top of the distribution curves are not available. Nevertheless, it has become the custom in electrochemistry and photoelectrochemistry to apply a pictorial representation of the energy dependence of the rate constants at electrodes in the form of Gerischer's distribution curves[1,3] when discussing electrode kinetics. The actual time scale of the rae constants represented by these distribution curves is generally neglected. In this paper we report time-resolved measurements that reveal the time scale corresponding to the maximum of Gerischer's distribution curve, i.e., the so-called activationless reaction (zero activation energy) at semiconductor electrodes.

The maximum rate constant is controlled by a typical frequency in the range of 10^{12} s^{-1} when the reaction follows an adiabatic path.[7,11] For even stronger electronic coupling, light-induced electron transfer can be still faster and can proceed from each excited vibrational level in competition with vibrational relaxation in the adsorbed molecule, leading to a nonexponential decay law.[1] Electron injection is irreversible due to extremely fast scattering with phonon creation[12] by the hot electron. On the other hand, for a nonadiabatic reaction path the maximum of Gerischer's distribution curve would correspond to a much slower time scale, e.g., nanosecond, and would thus be of the same order of magnitude as the radiative decay channel of a typical electronic excited state of a dye molecule.

It is at hand to perform an experiment with dye monomers adsorbed on a semiconductor electrode where the ground-state standard oxidation potential (E_{D/D^+} falls into the band gap and the fictitious standard oxidation potential in the excited singlet state ($E_{D/D^+} + h\nu_{0,0}$)[13] lies more than the reorganization energy (λ) above the edge (E_c of the wide[15] conduction band such that the maximum of Gerischer's distribution curve lies above the edge of the conduction band. This way an activationless reaction can be automatically realized by coupling neighboring unoccupied electronic levels in the wide conduction band to the adsorbed dye monomer promoted to its excited singlet state. The above described energetic situation[14] is illustrated in Figure 1. It is assumed that a short laser pulse with energy $h\nu_1$ promotes the level at the maximum of Gerischer's distribution curve to its first excited singlet state. This leads in general also to vibrational excitation. In the rate constants scheme in Figure 1, it is assumed that thermalization of the electronically excited adsorbed molecule (k_{relax}) precedes electron injection (k^* red). This injection process is irreversible due to translational motion and relaxation[15] of the hot electron in the conduction band (k_{rel}). Until now, there is no detailed theoretical model available for the injection process, i.e., the coupling of the orbitals of the excited adsorbed molecule to those on the surface of the semiconductor and for the subsequent

† Presented in part at the International Conference on "Chemistry and Physics of Electrified Interfaces", Bologna, Aug 1988.

‡ Fitz-Haber-Institut der Max-Planck-Gesellschaft.

§ E. I. du Pont de Nemours & Co.

(1) Gerischer, H. *Z. Phys. Chem. (Munich)* **1960**, *26*, 223; **1960**, *26*, 325; **1961**, *27*, 48.

(2) Gerischer, H. In *Physical Chemistry*, Vol. IX A, Eyring, H., Henderson, D., Jost, W., Eds.; Academic Press: New York, 1970; Vol. IX A, p 463.

(3) Gerischer, H.; Willig, F. In *Topics in Current Chemistry*; Boschke, F., Ed.; Springer: Berlin, 1976; Vol. 61, p 31.

(4) Buhks, E.; Williams, F. *Proc. Electrochem. Soc.* **1982**, *82-83*, 1.

(5) Ulstrup, J. *Charge Transfer Processes in Condensed Media*; Springer: Berlin, 1979.

(6) Marcus, R. A. *J. Chem. Phys.* **1980**, *43*, 679.

(7) Levich, V. G. In *Advances in Electrochemistry and Electrochemical Engineering*; Delahay, P., Tobias, C., Eds.; J. Wiley: New York, 1966; Vol. 4, p 249.

(8) Efrima, S.; Bixon, M. *Chem. Phys. Lett.* **1974**, *25*, 34; *Chem. Phys. A76*, *13*, 447.

(9) Ulstrup, J.; Jortner, J. *J. Chem. Phys.* **1975**, *63*, 4358.

(10) Schmickler, W. *J. Chem. Soc. Faraday Trans.* **1976**, *72*, 307.

(11) Bixon, M.; Jortner, J. *Faraday Discuss. Chem. Soc.* **1982**, *74*, 17.

(12) Tang, C. L.; Erskine, D. J. *Phys. Rev. Lett.* **1983**, *51*, 840.

(13) Leonhardt, H.; Weller, A. *Ber. Bunsen-Ges. Phys. Chem.* **1963**, *67*, 791.

(14) Gerischer, H. *Photochem. Photobiol.* **1972**, *16*, 243. It should be noticed that the "photocurrents" in this paper are "partial photocurrents" ($J_p \sim k_e$) proportional to the rate constant of electron transfer from the excited dye state (k_e), whereas the actual observed stationary photocurrent ($j \sim P_e$) is proportional to the probability of electron transfer (P_e), i.e., in the simplest case to a branching ratio of rate constants ($P_e = k_e/k_e + k_c$, where k_c collects all the rate constants of the competing reaction channels).

(15) Madelung, O., Ed. *Landolt-Börnstein*; Springer: Berlin, 1983; Vol. III/17 f, p 208. Fivaz, R. C.; Schmid, Ph. E. In *Physics and Chemistry of Materials with Layered Structures*; Lee, P. A., Ed.; Reidel Publishing Co.: Dordrecht, 1976; Vol. IV, p 343.

0002-7863/90/1512-2702$02.50/0

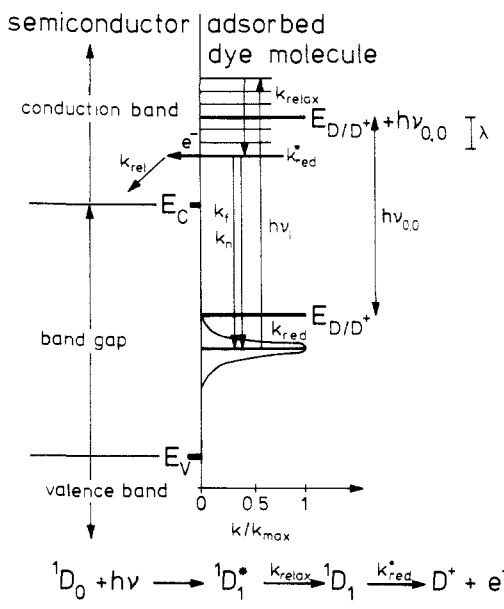

Figure 1. Scheme illustrating the experiment described in this paper to determine the time scale of electron transfer at the top of Gerischer's distribution curve.[1-3] The reaction sequence is given at the bottom, where k_{relax} refers to vibrational relaxation in the excited singlet state of the adsorbed dye molecule and the other symbols have their usual meaning.

release of a hot electron that undergoes elastic and inelastic scattering in the conduction band. It is clear from Figure 1 that such a system is ideally suited for an experiment that can reveal the time scale of the maximum rate constant at the top of Gerischer's distribution curve. In this experiment electron injection from the excited adsorbed dye monomers competes with the reaction channels for relaxation to the ground state. The fluorescence decay is the measured signal. The latter is controlled by electron injection at the maximum of the distribution curve if this rate constant is much faster than those in the competing radiative and nonradiative decay channels (k_f and k_n) of the excited singlet state of the monomers. The result of such an experiment in a well-defined experimental system is described below, showing that the maximum of Gerischer's distribution curve corresponds in this sytem to a reaction faster than 10 ps and thus most likely follows an adiabatic reaction path. The implication of this result will be discussed together with earlier experimental evidence for the value of the rate constant at the maximum of Gerischer's distribution curve.

Experimental Section

Fluorescence decay curves were measured with a Synchroscan streak camera (Hadland Imacon 500). Figure 2 shows the setup. The laser pulses were generated from a mode-locked argon ion laser (Spectraphysics 171) driving a dye laser with rhodamine 6G jet (Spectraphysics 375) with a cavity dumper (Spectraphysics 344S). The laser system was aligned for a half-width (fwhmh) of 5 ps as measured with an autocorrelator (Spectraphysics 409). The pulse train was checked with a fast photodiode. The system was optimized to obtain a good apparent pulse shape, measured with the Synchroscan streak camera, half-width between 12 ps for a single scan and 23 ps for long integration of a weak signal. Notice the greater jitter in the system with a cavity dumper compared to 7 ps measured with the streak camera for the synchronously pumped dye laser pulse train. The high repetition rate of the latter cannot be used for time-resolved single-photon counting that we apply routinely to measure long decay curves. Laser stray light was reduced by a close to 90° arrangement of laser beam and fluorescence detector and was totally eliminated with a series of cutoff filters, i.e., 3 OG 630 and 1 OG 610 (Schott). Each laser pulse contained 10^{10} photons. It was further attenuated by up to a factor of 100 with neutral gray density filters, to check on the linearity of the signals. The wavelength of the laser beam was fixed at 605 nm. After the spectral and optical alignment, the fluorescence decay measurements were carried out at a freshly cleaved surface of the SnS_2 electrode.[16]

(16) Parkinson, B. A. *Langmuir* **1988**, *4*, 967.

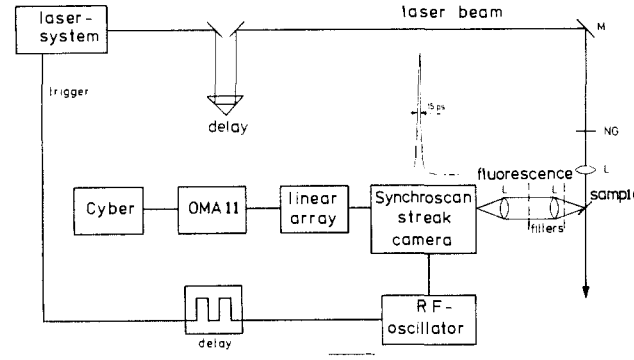

Figure 2. Experimental setup for measuring the fluorescence decay of a small number of dye molecules. Laser pulses were generated with repetition frequencies between 4 MHz and single shot, wavelength of 605 nm, and half-width (fwhmh) of 5 ps. The individual laser pulse contained typically 10^{10} photons and was often further attenuated in the experiment. The time dependence of the incident repetitive fluorescence signal was converted into a spatial dependence at the exit of the synchronously recording streak camera. Many identical signals were averaged in each measurement. The apparent laser pulse, as measured with the streak camera, was broadened due to several jitter sources in the system. It is shown on top of the symbol for the streak camera.

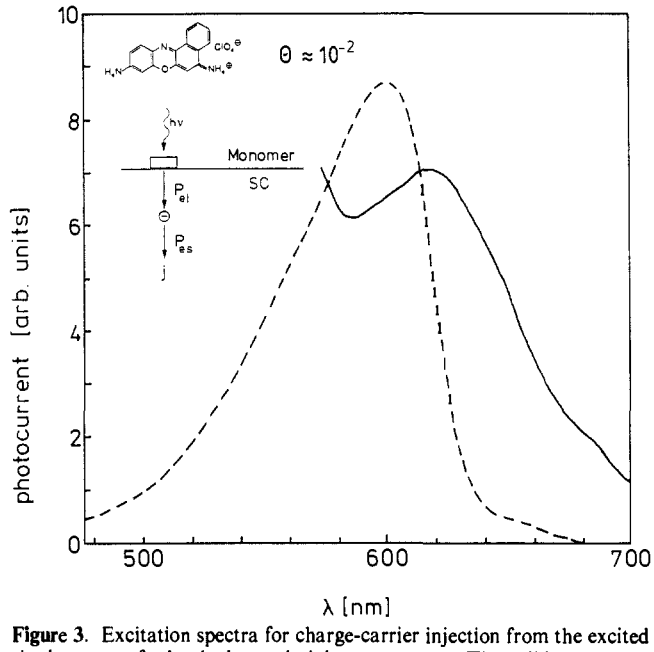

Figure 3. Excitation spectra for charge-carrier injection from the excited singlet state of adsorbed cresyl violet monomers. The solid curve represents the *n*-SnS_2 electrode[15] in contact with 3×10^{-8} M aqueous solution of the dye, and the dashed curve represents the anthracene single-crystal electrode in contact with 1×10^{-8} M aqueous solution of the dye.

Prior to the fluorescence decay measurements, it was checked and confirmed at the same SnS_2 electrode that the stationary injection yield was close to one electron in the external circuit per photon absorbed by the cresyl violet monomers as has been reported before by Parkinson.[16] Current-voltage curves and excitation spectra of the photocurrents were measured with a conventional experimental setup.[3]

Fluorescence spectra were checked in a rough manner with interference filters. However, to measure the fast weak decay signals, we applied only cutoff filters. It was carefully checked that laser stray light was completely blocked. Spectral diffusion and energy migration are negligible at coverages around 10^{-2}. It plays a dominant role though at coverages ≥ 0.1, and the corresponding fluorescence decay curves are rather involved. The complicated kinetic situation in the adsorbed dye layer at higher coverages will be discussed elsewhere. Cresyl violet was purchased from λ-Physik; *n*-SnS_2 electrodes were grown as described before.[16]

Experimental Results

The system is comprised of cresyl violet molecules adsorbed from extremely dilute aqueous solutions onto the sulfur van der Waals surface of moderately doped *n*-SnS_2.[16] Renewal of the

surface was extremely simple; i.e., the old surface was gently peeled off. The newly exposed surface is known to be very inert[16,17] against corrosion. Figure 3 shows excitation spectra of charge injection currents for cresyl violet monomers adsorbed on van der Waals surfaces. The solid curve corresponds to electron injection into the sulfur surface of n-SnS_2 in contact with an aqueous solution of 3×10^{-8} M cresyl violet and 1 M KCl. The dashed curve corresponds to hole injection into the ab surface of an ultrapure anthracene sublimation crystal in contact with an aqueous solution of 1×10^{-8} M cresyl violet. The latter spectrum is identical with the absorption spectrum of the cresyl violet monomer ($\leq 10^{-7}$ M) in aqueous solution except for a red shift by 4 nm in this excitation spectrum. The rise to the left in the solid curve is caused by the superimposed absorption edge of SnS_2. It is clear from Figure 3 that the red shift is much stronger (650 cm^{-1}) for cresyl violet adsorbed on the sulfur van der Waals surface of single crystal SnS_2 than the shift (112 cm^{-1}) on the van der Waals ab plane of the anthracene crystal. With increasing concentration of cresyl violet in the aqueous contact solution, the current yield, i.e., electrons in the external circuit per incident photon at 620 nm, reaches a value of 2% in the micromolar concentration range where a change in slope occurs[16] in the yield versus dye concentration plot. This change in slope has been attributed to the completion of a monolayer, since it coincides with a number of injected electrons in accord with the number of photons absorbed by a densely packed monolayer of dye molecules lying flat on the surface. This is only an approximation, as will be discussed elsewhere. It is sufficient for a qualitative estimate of the dye coverage.

The adsorption procedure for all fluorescence measurements was extremely simple. A droplet of the aqueous dye solution was released from a syringe onto the freshly exposed sulfur surface of SnS_2. It formed an almost hemispherical droplet of about 2-mm diameter on the hydrophobic sulfur surface. This droplet was left there for 10 min and was then removed by its being soaked off the surface into Kleenex paper. The fluorescence decay curve was measured immediately afterward and also several times at later time intervals. Finally, it was remeasured the next day. The same procedure was repeated with a higher dye concentration on the same spot where the first droplet had been placed and so on. The measurements were repeated with a different procedure where each new dye concentration was measured on a freshly peeled surface. The results of both procedures were identical. To check on reversible or irreversible bleaching, we varied the exposure time to the laser beam. No decrease in the signal height was detected with repetition rate of 800 kHz, 10^{10} photons/laser pulse, and an exposure time within 1 s. A decrease in the signal height was only observed for an exposure time of several minutes at a higher doped n-SnS_2 electrode with a slow recovery in the dark. This effect is tentatively ascribed to trapping of the injected electrons in deep traps. The absence of a bleaching effect under the above experimental conditions at the moderately doped n-SnS_2 electrodes is compatible with an average recombination time between injected electrons and oxidized parent dye molecules that is 1 ms or shorter.

The fluorescence decay curves for the very dilute dye solution (3×10^{-8} M) measured immediately after the adsorption procedure (wet condition) and 1 day later (dry condition) are shown as Figure 4, parts b and c, respectively. Figure 4a shows the apparent shape of the laser pulse. Parts d and e of Figure 4 represent the analogous fluorescence decay signals measured after contact formation for 10 min with a 10^{-7} M aqueous solution of cresyl violet in the wet and dry condition, respectively. Figure 4f shows the signal after contact formation for 10 min with a 3×10^{-5} M aqueous solution of the dye. In the latter case there was no noticeable difference in this time window for the signals corresponding to the wet and dry conditions. Since the decay in Figure 4f is very long, this measurement is not very meaningful in the time window of the streak camera. However, it is sufficient to illustrate the much slower fluorescence decay in the presence

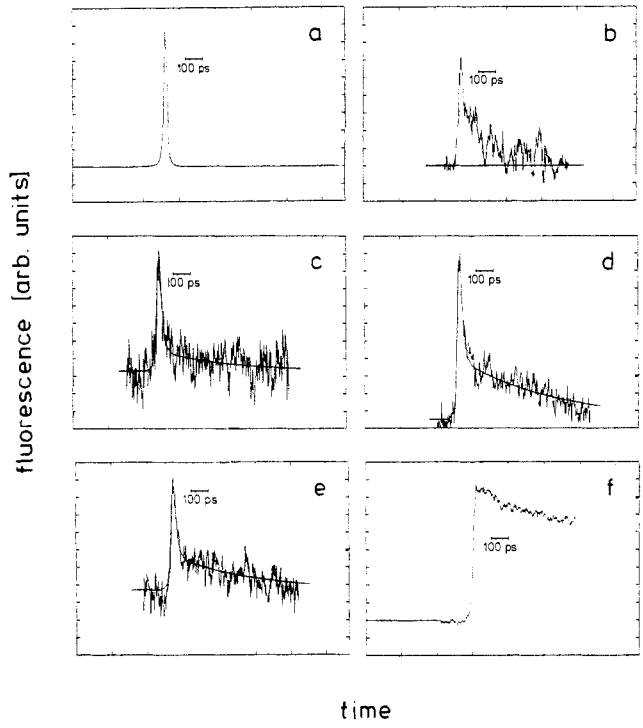

Figure 4. Fluorescence decay curves of cresyl violet monomers adsorbed from aqueous solution on the sulfur cleavage plane of single-crystal n-SnS_2. Curve a gives the apparent shape of the laser pulse measured under the excitation conditions with the streak camera, curve b is the signal due to adsorption for 10 min from a 3×10^{-8} M cresyl violet droplet of aqueous solution (wet condition, see text), and curve c is the corresponding signal in the dry condition (see text). Curves d and e are the signals obtained for adsorption from a droplet of 1×10^{-7} M cresyl violet measured in the wet and dry conditions, respectively. Curve f is the signal obtained for adsorption from a droplet of 3×10^{-5} M aqueous solution cresyl violet. The fast component with time constant <10 ps in Figure 4b–e is controlled by electron injection from the excited singlet state of adsorbed cresyl violet monomers. The solid lines in curves c–e are calculated curves (see text).

of cresyl violet aggregates that has been observed already before at higher dye coverages.[18] Fluorescence decay of cresyl violet molecules in aqueous solution is even slower than in Figure 4f. The signal to noise ratio improved considerably from Figure 4b (3×10^{-8} M dye solution) to Figure 4d (1×10^{-7} M dye solution) due to the expected increase in the dye coverage by about a factor of 3. This concentration range is still acceptable since the fast signal of the isolated monomers can be clearly distinguished from the slow signal in the presence of aggregates. Also in the case of the very noisy signals in Figure 4b,c, we made sure that we did not measure stray light of the laser pulse. To this end, some of the filters that were blocking the laser stray light were intentionally removed to obtain a 100 times stronger stray light pulse superimposed on the actual fluorescence signal from the dye monomers. Now the stray light of the laser pulse was attenuated again in calibrated steps by reinserting blocking filters. In the final situation with all the blocking filters inserted, the stray light pulse from the laser was at least 10^3 times smaller than the fast signal shown in Figure 4b,c. In view of the charge carrier injection yield close to 1, we can attribute the fast decay to electron injection from the excited singlet state of adsorbed cresyl violet monomers. At this point it is important to notice that fluorescence decay of adsorbed dye molecules becomes very slow with decreasing dye coverage when the surface does not facilitate a fast reaction for the excited singlet state of the dye monomer.[19] Cresyl violet monomers embedded in amourphous silica showed a very narrow spectral hole of about 1 GHz,[20] corresponding to a long lifetime

(17) Stickney, J. L.; Rosasco, S. D.; Schardt, B. C.; Solomun, T.; Hubbard, A. T.; Parkinson, B. A. *Surf. Sci.* **1984**, *136*, 15.

(18) Anfinrud, P.; Crachel, R. L.; Struve, W. S. *J. Phys. Chem.* **1984**, *88*, 5873.

(19) Willig, F.; Blumen, A.; Zumofen, G. *Chem. Phys. Lett.* **1984**, *108*, 222.

with a fluorescence decay of about 1 ns.

Identification of the fluorescence decay curves with the speed of electron transfer as represented by the maximum in Gerischer's distribution curves is only meaningful for electron injection from dye monomers. Therefore, our measurements were carried out also at the lowest dye coverages where a decay signal was still experimentally accessible, since trapping of the excitation energy at dye aggregates leads to additional complicated features of the fluorescence decay curves.[18,19] Cresyl violet was chosen for this experiment since fluorescence decay in the presence of cresyl violet aggregates is unusually slow compared to the effect of aggregates on fluorescence decay in the case of many other adsorbed dye molecules, e.g., in the case of adsorbed rhodamine B.[19] At the very low coverage achieved with 3×10^{-8} M rhodamine B we measured a similar extremely short fluorescence decay signal of the monomers adsorbed on SnS_2 as the peaks in Figure 4b,c for cresyl violet monomers. The solid curves in Figure 4c–e are least-squares computer fits to the experimental decay signals applying the following simple model that is further explained in the Discussion

$$F(t) = \int_0^t \phi(t - t')(1 - e^{-t'/t_r})(a_1 e^{-t'/t_1} + a_2 e^{-t'/t_2})\, dt' \quad (1)$$

$\phi(t)$ = experimental response signal of the measuring system to the laser pulse. Thus, it contains the convolution of the actual laser pulse with the instrumental response function. The rise of the signal is determined by the vibrational relaxation time τ_r in the electronic excited singlet state $^1S_1$ of the adsorbed dye monomer. We have chosen τ_r = 500 fs, inspired by experimental results on vibrational relaxation in the $^1S_1$ state of other dye molecules.[21] This way we have assumed that the reaction occurs from the thermalized $^1S_1$ state. Fluorescence decay due to electron injection from the monomers was dominant in all cases; i.e., a_1 = 0.96 in Figure 4c and a_1 = 0.88 and 0.91 in Figure 4, parts d and e, respectively, with $a_1 + a_2 = 1$. We did not succeed until now in preparing a comparable semiconductor electrode where electron injection does not occur. GaS with an upward-shifted conduction band contained, unfortunately, fluorescing impurities. Therefore, we could not assess with sufficient certainty whether a possible depression in the height of the peaks in Figure 4b–e had occurred with respect to the initial fluorescence signal of a noninjecting system. We assumed for the numerical fits that there is virtually no depression in the initial height of the peaks. With this assumption we obtained only an upper limit for the short lifetime from the computed least-squares deviation curves; i.e., $\tau_1 \leq 10$ ps. The slow-decay component with τ_2 contributed at the lowest coverage with a_2 = 0.04 (Figure 4b,c); it rose to a_2 = 0.12 and 0.09 in parts d and e of Figure 4 and continued to grow with increasing dye coverage (not shown) to cover completely the fast component. An example for the latter situation is shown in Figure 4f. In the short time window of our measurement (Figure 4b–e) the slow component decayed with $\tau_2 \approx$ 400–500 ps; i.e., the fits gave 360 ps in the time window of Figure 4c, 530 ps in Figure 4d, and 415 ps in Figure 4e. In accordance with the systematic trend, i.e., increase in a_2 with rising coverage, displayed in Figure 4b–f, we attribute the slow signal to fluorescence decay in the presence of aggregates. This slow decay originated most probably in tiny dye islands on the surface that contained dye aggregates as traps. In the present context, however, we are only interested in the fast signal with $\tau_1 \leq 10$ ps, stemming from the adsorbed monomers that can be identified with electron injection at the top of Gerischer's distribution curve.

A rough estimate for monolayer equivalent coverage of cresyl violet at SnS_2 has been made. Accordingly, several micromolar concentration of cresyl violet in aqueous solution lead to a dye coverage in the range of 1.[16] This suggests a dye coverage in the range of 10^{-2} for adsorption from the 3×10^{-8} M aqueous solution of cresyl violet. Adsorption with a sticking coefficient 1 of all the molecules within the effective diffusion length of about 0.05 cm, corresponding to 10-min contact time for a 3×10^{-8} M solution, predicts a coverage of the same order of magnitude. Therefore, curves b and c in Figure 4 correspond approximately to a coverage of 10^{-2}. In accordance with the fluorescence decay curves in Figure 4 we can assume that an appreciable percentage of cresyl violet molecules is adsorbed as dye monomers at such a low dye coverage, giving rise to the fast components in Figure 4b–e.

Discussion

The system cresyl violet monomers on the surface of SnS_2 investigated in this paper fulfill $E_{D/D^+} + h\nu_{0,0} - E_c > \lambda$ (Figure 1) and allow for activationless electron injection, i.e., with zero activation energy into the wide conduction band[15] of SnS_2. The edge of the conduction band lies at about E_c = 0 V versus NHE for SnS_2.[16] The oxidation potential is E_{D/D^+} = 1.15[16] versus NHE for cresyl violet, and $h\nu_{0,0}$ estimated from absorpton and fluorescence spectra in aqueous solution is 1.97 eV. Thus, the oxidation potential of the excited singlet states lies 0.8 eV above the band edge E_c. We do not know the shift in E_{D/D^+} for the adsorbed molecules, but this downhill energy difference is much larger than a reasonable value (0.4 eV) for the reorganization energy of these large dye molecules.[22] Thus, the redox energy level of the excited singlet state of the dye provides for an activationless electron transfer reaction. It is straightforward to derive from the rate constants scheme in Figure 1 the time dependence for the fluorescence decay as given in Figure 1 with $a_1 = 1$ and $a_2 = 0$. We assumed here that thermalization (k_{relax}) precedes electron injection. This assumption is not unambiguous on the basis of our present experimental results. However, the observed relatively strong initial signal heights compared to fluorescence emission from Langmuir–Blodgett monolayers diluted to $\theta = 10^{-2}$ dye coverage appear to support this assumption. From the solution of the rate constants model we identify $1/\tau_r = k_{relax} - (k^*_{red} + k_f + k_n)$ and $1/\tau_1 = k^*_{red} + k_f + k_n$ with the usual notation and the meaning explained in Figure 1. Fast translation motion and relaxation of the hot electron[12] make the injection process irreversible. There is also an intramolecular and environmental (solvent) relaxation after the electron has left the adsorbed molecule to produce the oxidized state. As already mentioned in the introduction, a theoretical model is still missing for the injection process. It should describe orbital coupling for the excited adsorbed molecule, generation and scattering of the hot electron, and the relaxation of the oxidized molecule. It is known from spectral hole burning experiments that cresyl violet monomers decay slowly, $k_f + k_n \approx 10^9$ s^{-1}, on an inert surface.[20] We, therefore, identify the fast-decaying component in Figure 4b–e with the electron injection process $1/\tau_1 = k^*_{red}$. For the numerical fits we have used in eq 1, $1/\tau_r = 2 \times 10^{12}$ s^{-1} on the basis of recent experimental evidence.[21] The decay curves in Figure 4 contain a second much slower component that is rising with increasing dye coverage. It has to be ascribed to fluorescence decay in tiny dye islands where aggregates function as traps.[18,19] Our present investigation aimed specifically at measuring the monomer fluorescence decay that can be identified with electron injection was therefore extended to the lowest dye coverages where a meaningful decay signal can still be measured. For our least-squares deviation fits (solid curves in Figure 4), we always used the lowest possible value for k^*_{red}. This is a precaution since we had no unambiguous information on the height of the initial signal compared to a noninjecting system. Thus, our fits to the experimental decay curves gave only a lower limit $k^{*red} > 10^{11}$ s^{-1}. With use of site-selective laser excitation it should be possible to determine k^*_{red}, at least at very low temperatures, from the line width in a spectral hole burning experiment. Realistic injection speeds between 10 fs and 10 ps correspond to half-widths between 500 and 0.5 cm^{-1}. Such widths are easily resolved in spectral hole burning experiments. The fast decay times due to electron injection can also be directly time resolved provided the sensitivity and bleaching problems in such systems can be overcome also in

(20) Locher, R.; Renn, A.; Wild, U. P. *Chem. Phys. Lett.* **1987**, *138*, 405.
(21) Angel, G.; Gagel, R.; Laübereau, A. *Chem. Phys.* **1989**, *131*, 129.
(22) Van Duyne, R. P.; Fischer, S. F. *Chem. pHys.* **1974**, *5*, 183.

the shorter time windows. It should be noticed here that the resolution of spectroscopic methods currently applied in surface science is much lower than, e.g., in spectral hole burning experiments and too low for the above most interesting time windows of fast electron-transfer reactions.

The measured dominant decay time, ≤ 10 ps, shows that the electron injection mechanism is adiabatic or lies at least at the borderline between a nonadiabatic and an adiabatic reaction path. There is no experimental information available on the magnitude of the electron-transfer integral. For cresyl violet at very low coverage of about 10^{-2} on SnS_2, the peak of the excitation spectrum of the photocurrent is red shifted by 650 cm^{-1} versus the absorption peak in the adjacent solution or 538 cm^{-1} versus the peak of the injection current into an anthracene crystal (Figure 3). However, there is no straightforward relationship between this red shift for the adsorbed dye monomer and the value of the electron-transfer integral.

A theoretical estimate is also not available for the electron-transfer integral in the present system. At the one extreme, the resonance width of alkali atoms on a jellium surface has been calculated recently in the range between 0.3 and 3 eV, depending on the hybrid orbital.[23] At the other extreme, the electron-transfer integral between anthracene molecules in the crystal has been calculated in the range of 0.1 eV.[24] It appears reasonable to assume that the value of the electron-transfer integral is larger for the present system than in the latter example. The reaction proceeds along an adiabatic path when the Landau–Zener parameter is greater than 1.[7,25] For a reaction between molecules this parameter has been estimated as

$$Y = \frac{2\pi V^2}{\hbar\omega(2\lambda k_B T)^{1/2}} \qquad (2)^{26}$$

With $\lambda = 0.4$ eV for the rigid dye molecule cresyl violet[22] and a reasonable dominating oscillator for the slow coordinates of $\hbar\omega \leq 100$ cm^{-1}, the reaction is adiabatic already for $V \geq 100$ cm^{-1} or 0.012 eV. According to the above estimates for V this should be easily fulfilled in the present system.

There were several earlier measurements of the fluorescence decay of adsorbed dye molecules on inorganic semiconductor electrodes that were ascribed to electron injection.[27a-i] The decay constants varied over a wide range in these measurements, even for comparable systems, where the maximum of Gerischer's distribution curve was expected to lie well above the edge of the conduction band, e.g., 38 ps for rhodamine B on SnO_2,[27g] 410 ps for rhodamine B on SnO_2,[27c] 238 ps for chlorophyllin on colloidal TiO_2,[27e] and 770 ps for dry $[Ru(bipy)_3]^{2+}$ on TiO_2 powder.[27i] Decay times as short as 680[27c] and 400 ps[27f] have been measured already for dye monomers on glass slides. The latter are due to reactions of the excited dye molecules with local sites and cannot be ascribed to electron transfer into a wide conduction band. However, the correspondence of one injected electron in the stationary photocurrent to one photon absorbed in the dye layer has not been checked in the above systems.[27a-i] This 1 to 1 correspondence is essential to ascribe the measured fluorescence decay unambiguously to the electron injection channel.

In many of the earlier measurements the dye coverage was not sufficiently low but was chosen in the range of the photocurrent maximum versus dye concentration curve, i.e., at $\theta > 0.1$. It is already obvious from the trend in Figure 4b–f that dye coverages ≥ 0.1 correspond in general to very complicated decay kinetics for the excited state generated by photon absorption in such a dye layer. All of the earlier experiments showed a slower fluorescence decay in the adsorbed dye layer than the present experiments obtained with adsorbed dye monomers at about $\theta = 10^{-2}$, at a clean inert freshly prepared surface. There are many reasons for a slowing in the speed of electron injection, among them a corrosion layer on the semiconductor surface, an inbetween water layer, and a trapping of the excitation energy at dye aggregates that do not couple directly to the semiconductor surface.

Ultrafast fluorescence decay of the adsorbed dye molecules together with a stationary current yield of one injected electron for one excited adsorbed dye monomer, as is valid in the present system, is still compatible with the assumption of an undetected intermediate reaction step. In this scheme fluorescence decay is due to ultrafast electron transfer to a local state on the semiconductor surface from where the electron escapes into the conduction band and is further away from the surface before recombination can occur from the local reduced state to the oxidized parent dye molecule. The maximum of Gerischer's distribution curve corresponds then to the first step in this reaction sequence. At present there are no time-resolved experiments available that distinguish between such a reaction sequence and direct electron injection into the wide conduction band. However, the ultrafast fluorescence decay observed in the present system supports direct injection into the wide conduction band. In the case of the intermediate step, a by chance suitable energetic position of the local state would be required near the top of Gerischer's distribution curve together with other suitable rate constants to make the reaction sequence via the local surface state an efficient injection path.

Extrapolation procedures can be applied to estimate from stationary results the absolute value of rate constant at the peak of Gerischer's distribution curve. We will quote here two representative examples: Gomes et al.[28] measured the voltage dependence of the dark injection current of the redox couple $Fe(CN)_6^{3-/4-}$ into n-ZnO and determined the rate constant of 10^{-18} cm^4 s^{-1} at pH = 9.2. They estimated that the maximum of Gerischer's distribution curve for the reduction of the oxidized species should lie near the edge of the conduction band E_c. Taking a reasonable reaction distance in the range of several angstroms, their rate constant would indeed correspond to a reaction time in the picosecond time domain, in qualitative agreement with the result obtained here in a direct time-resolved measurement at a different better defined experimental system.

Not all of the electron injection reactions are expected to follow an adiabatic path with the redox reactant only a few angstroms away from a sufficiently clean electrode. For example electron transfer through an inefficient ligand bridge can significantly reduce the electron-transfer integral and thus lead to a nonadiabatic reaction with the maximum of Gerischer's distribution curve falling for example into the nanosecond time domain. We expect, however, that the majority of cases will follow the adiabatic path or will be fairly close to it on a clean substrate without intermittant water or corrosion layer.

There is an interesting implication of the present experimental result also for redox reactions at metal electrodes and the respective Gerischer distribution curves. The highest direct-time resolution reported until now for redox reactions at metal electrodes in the dark corresponds to 10 ns and longer.[29] An adiabatic redox reaction with zero activation energy would be faster than 10 ps as is borne out by the result shown in this paper. Thus, time-resolved measurements with 10-ns resolution can resolve the

(23) Nordlander, P.; Tully, J. C. *Phys. Rev. Lett.* **1988**, *61*, 990.
(24) Silbey, R.; Jortner, J.; Rice, S. A.; Vala, M. T. *J. Chem. Phys.* **1965**, *42*, 733; **1965**, *43*, 2925.
(25) Landau, L. *Phys. Z. Sowjetunion* **1932**, *2*, 46. Zener, C. *Proc. R. Soc. London, A* **1932**, *137*, 696.
(26) Bixon, M.; Jortner, J.; Plato, M.; Michel-Beyerle, M. E. In *Photosynthetic Bacterial Reaction Center*; Breton, J., Vermiglio, A., Eds.; NATO ASI Series; Plenum Press: New York, 1988; p 399.
(27) (a) Itoh, K.; Chiyokawa, Y.; Nakao, M.; Honda, K. *J. Am. Chem. Soc.* **1984**, *106*, 1620. (b) Liang, Y.; Ponte Goncalves, A. M.; Negus, D. K. *J. Phys. Chem.* **1983**, *87*, 1. (c) Liang, Y.; Ponte Goncalves, A. M. *J. Phys. Chem.* **1985**, *89*, 3290. (d) Crackel, R. L.; Struve, W. S. *Chem. Phys. Lett.* **1985**, *120*, 473. (e) Kamat, P. V.; Chauvet, J.-P.; Fessenden, R. W. *J. Phys. Chem.* **1986**, *90*, 1389. (f) Hashimoto, K.; Hiramoto, H.; Kajiwara, T.; Sakata, T. *J. Phys. Chem.* **1988**, *92*, 4636. (g) Hashimoto, K.; Hiramoto, M.; Skata, T. *J. Phys. Chem.* **1988**, *92*, 4272. (h) Hashimoto, K.; Hiramoto, M.; Sakata, T. *Chem. Phys. Lett.* **1988**, *148*, 215. (i) Hashimoto, K.; Hiramoto, M.; Lever, A. B.; Sakata, T. *J. Phys. Chem.* **1988**, *92*, 1016. (k) Eichberger, R.; Willig, F. *Chem. Phys.*, in press.
(28) Vanden Berghe, R. L.; Cardon, F.; Gomes, W. P. *Surf. Sci.* **1973**, *39*, 368.
(29) Bernstein, C.; Vielstich, W. *Proc. Electrochem. Soc.* **1980**, *80–83*, 351.

corresponding Gerischer distribution curve only up to 10^{-3} of its maximum value, i.e., to a value where the customary linear representation of Gerischer's distribution curve still does not rise above the zero line. Considering the activation energy ($\lambda/4$) for the exchange current[1,9] at a metal electrode, this implies also that time-resolved measurements in the dark with 10-ns time resolution can only resolve adiabatic exchange currents with large reorganization energies, $\lambda > 0.75$ eV. The present knowledge, about the line shape corresponding to the energy dependence of the rate constant equivalent to Gerischer's distribution curve, is not sufficient for any molecule or redox ion to extrapolate from a measured value that is a factor of 10^{-3} smaller all the way up to the maximum value. The experiment described here gives a clear indication of the relevant time scale (<10 ps) at the maximum of Gerischer's distribution curve that is widely used as pictorial representation of the energy dependence of electron-transfer rate constants at electrodes.

Acknowledgment. We thank two members of our group for their invaluable help in this work, J. Lehnert for excellent technical assistance and R. Kietzmann for carrying out the computer fits. We are grateful to the Fonds der Chemischen Industrie for financial support.

Registry No. *n*-SnS_2, 1315-01-1; cresyl violet, 18472-84-4.

A Spectroscopic Study of the Interaction of D- and L-*N*-(3,5-Dinitrobenzoyl)valine Methyl Ester with *n*-Butylamide of (*S*)-2-[(Phenylcarbamoyl)oxy]propionic Acid: Direct Evidence for a Chromatographic Chiral Recognition Rationale

Gloria Uccello-Barretta, Carlo Rosini, Dario Pini, and Piero Salvadori*

Contribution from the Centro di Studio del CNR per le Macromolecole Stereordinate ed Otticamente Attive, Dipartimento di Chimica e Chimica Industriale, via Risorgimento 35, 56126 Pisa, Italy. *Received March 3, 1989*

Abstract: The *n*-butylamide of (*S*)-2-[(phenylcarbamoyl)oxy]propionic acid forms diastereoisomeric adducts with the two antipodes of *N*-(3,5-dinitrobenzoyl)valine methyl ester. Their structures in solution have been studied by ^1H, ^{13}C, and ^{15}N NMR spectroscopy, and by their comparison it has been possible to gain some insights into the chiral recognition mechanism by which the enantiomers of *N*-(3,5-dinitrobenzoyl)amino acid methyl esters are separated by use of a chiral stationary phase obtained by immobilizing (*S*)-2-[(phenylcarbamoyl)oxy]propionic acid onto γ-aminopropylsilica gel.

Recently we reported[1] the preparation of a new chiral stationary phase (CSP) obtained by immobilizing (*S*)-2-[(phenylcarbamoyl)oxy]propionic acid (carbamalactic acid) on γ-aminopropylsilanized silica and its use for the chromatographic separation of *N*-(3,5-dinitrobenzoyl)amino acid methyl esters. As it has been pointed out by other authors[2] and ourselves,[3] it is possible to gain insights into the chiral recognition mechanism by studying the interactions between the chiral residue linked to the chromatographic support (assumed as a good, soluble model of the CSP) and the antipodes of a substrate which is resolved on the CSP itself.

We report here the results of a study of interactions occurring, in solution, between the *n*-butylamide of (*S*)-2-[(phenylcarbamoyl)oxy]propionic acid (CBL) and L- or D-*N*-(3,5-dinitrobenzoyl)valine methyl ester (L-Val or D-Val, respectively) (Chart I) using NMR spectroscopy. Although a number of methods for detecting diastereoisomeric interactions have been developed, NMR spectroscopy constitutes one of the more sensitive probes used to reveal[2] the occurrence of such interactions and, more importantly, to gain detailed information on their nature. The determination of the structure of the diastereoisomeric adducts, CBL/L-Val and CBL/D-Val, provides information on their relative stability, and then, assuming that these adducts are similar to the selector–selectand and complexes, elution orders can be rationalized and a chromatographic chiral recognition mechanism can be proposed.

Chart I

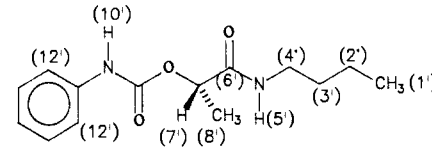

n-butylamide of (S)-2-(phenylcarbomoyloxy)propionic acid

(CBL)

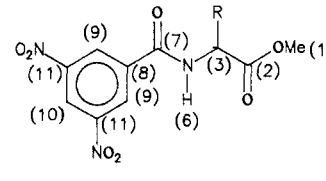

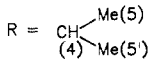

N-(3,5-dinitrobenzoyl)valine

methylester

(VAL)

Results and Discussion

Our recent investigations on the CSP derived from carbamalactic acid, undertaken to explore the dependence of chromatographic separation on the structure of the amino acid derivatives, demonstrated that the presence of 3,5-dinitrobenzoyl and methyl ester groups on the substrate is essential for the chiral recognition.[1]

(1) Salvadori, P.; Pini, D.; Rosini, C.; Uccello-Barretta, G.; Bertucci, C. *J. Chromatogr.* **1988**, *450*, 163.
(2) Pirkle, W. H.; Pochapsky, T. C. *J. Am. Chem. Soc.* **1987**, *109*, 5975 and ref 17 therein.
(3) Salvadori, P.; Rosini, C.; Pini, D.; Bertucci, C.; Altemura, P.; Uccello-Barretta, G.; Raffaelli, A. *Tetrahedron* **1987**, *43*, 4969.

0002-7863/90/1512-2707$02.50/0